



Significant Improvement of $\text{LiNi}_{0.8}\text{Co}_{0.15}\text{Al}_{0.05}\text{O}_2$ Cathodes at 60°C by SiO_2 Dry Coating for Li-Ion Batteries

Yonghyun Cho and Jaephil Cho^{*,z}

School of Energy Engineering, Ulsan National Institute of Science and Technology, Ulsan 689-798, Korea

The cycling performance of a $\text{LiNi}_{0.8}\text{Co}_{0.15}\text{Al}_{0.05}\text{O}_2$ cathode at 60°C was substantially improved by direct SiO_2 dry coating. The SiO_2 -coated cathode was obtained from firing of the mixture consisting of SiO_2 nanoparticles and the cathode powders with a weight ratio of 99:1 at 700°C for 5 h. The first discharge capacity of the coated cathode was 172 mAh/g, whereas the uncoated one showed 182 mAh/g at 60°C . However, the coulombic efficiency of the coated sample was 95%, which was 2% higher than that of the uncoated sample. Moreover, the discharge capacities of the coated cathode at 60°C was about 2.5 times larger than those of the uncoated sample at rates of 0.5 and 1C, showing 146 and 109 mA/g, respectively. This capacity improvement at 60°C is related to the fact that the highly distributed Si element near the surface, as a type of solid solution with $\text{LiNi}_{0.8}\text{Co}_{0.15}\text{Al}_{0.05}\text{O}_2$, diminishes the side reactions of the cathode and electrolyte at 60°C .

© 2010 The Electrochemical Society. [DOI: 10.1149/1.3363852] All rights reserved.

Manuscript submitted October 29, 2009; revised manuscript received February 16, 2010. Published April 15, 2010.

Conventional coating methods are wet-coating methods that use aqueous or nonaqueous solvents; however, these methods require additional mixing and drying processes.¹⁻⁸ As a consequence, a study of a simple dry-coating method that does not use a solvent has been initiated.⁹ Thus far, coated cathodes prepared by wet-coating methods have demonstrated greatly improved electrochemical performance at room temperature. The electrochemical cycling properties of coated cathodes at an elevated temperature, e.g., 60°C , are much more important than those at room temperature because the side reactions lead to cell swelling and deteriorated cycling performances. At elevated temperatures, catalytic side reactions between the electrode coating surface and the electrolytes can lead to an increased formation of a nonconducting solid electrolyte interface (SEI) layer, resulting in a rapid decrease in capacity. In this regard, few studies of Ni-rich based cathodes above 60°C have been reported.^{10,11} The $\text{LiNi}_{0.8}\text{Co}_{0.15}\text{Al}_{0.05}\text{O}_2$ cathode has been considered as a promising cathode material among other Ni-rich candidates because of its improved stability and electrochemical performance brought by Co and Al substitutions for Ni in LiNiO_2 . Because the radii of Co^{3+} and Al^{3+} are smaller than that of Ni^{3+} , the substitutions of these ions result in the shrinkage of the *a*-axis, which is considered to be the origin of stabilizing the layered structure. Despite such improvements, $\text{LiNi}_{0.8}\text{Co}_{0.15}\text{Al}_{0.05}\text{O}_2$ still has problems of capacity fade during storage and cycling at $>50^\circ\text{C}$.¹²

As the performance at an elevated temperature is greatly influenced by the coating material, coating candidates should be selected carefully. Previously, TiO_2 nanoparticle coating on LiCoO_2 cathodes by a dry-coating method showed comparable cycling performance to that at room temperature,⁹ but no studies of the cycling performance in the Ni-rich system above 60°C have been done.

This study reported the synthesis and electrochemical properties of the SiO_2 -coated $\text{LiNi}_{0.8}\text{Co}_{0.15}\text{Al}_{0.05}\text{O}_2$ cathode. A simple dry coating of SiO_2 nanoparticles on the cathode improved the cycling performance at 60°C compared to the uncoated and TiO_2 -coated samples.

Experimental

To prepare $\text{LiNi}_{0.8}\text{Co}_{0.15}\text{Al}_{0.05}\text{O}_2$, stoichiometric amounts of $\text{Ni}_{0.8}\text{Co}_{0.15}\text{Al}_{0.05}(\text{OH})_2$ (Ecopro, Korea) and $\text{LiOH}\cdot\text{H}_2\text{O}$ with a molar ratio of 1:1.03 (dried precursor: $\text{LiOH}\cdot\text{H}_2\text{O}$) were mixed and annealed at 750°C for 15 h. Coating concentration (1 wt %) was referred to when 1 g of SiO_2 or TiO_2 (the particle size was ~ 100 nm) and 100 g of $\text{LiNi}_{0.8}\text{Co}_{0.15}\text{Al}_{0.05}\text{O}_2$ were used. A PD96 power homogenizer (Laboratory Science, Korea) was used for the mixing of SiO_2 and cathode powders. The powders were dry-mixed

in a homogenizer for 2 h and fired at 700°C for 5 h in air to obtain coated cathodes. To test the cycle-life performance of each cathode material, a slurry was prepared by mixing the active material, super P carbon black, and a poly(vinylidene fluoride) binder with weight ratios of 94:3:3 in *N*-methyl-2-pyrrolidone. The amount of cathode materials was ~ 21 mg in the composite cathode. A lithium cell (2016R size) contained a test cathode, a lithium metal anode, a 15 μm thick microporous polyethylene separator, and an electrolyte solution of 1.03 M LiPF_6 in ethylene carbonate/dimethyl carbonate (1:1 vol %) (LG Chem., Korea). The amount of cathode materials was ~ 21 mg in the composite cathode. The 1C rate corresponded to 3.8 mA/cm^2 .

X-ray photoelectron spectroscopy (XPS) analyses were performed with a Thermo Scientific K-Alpha spectrometer using a monochromatic Al $\text{K}\alpha$ radiation of an energy beam (1486.6 eV). Spectra were recorded in the constant pass energy mode at 50.0 eV using a 30 μm diameter analysis area. For the depth profile, etch times of 0–285 s were used. Before etching, the surface of the electrode was covered with the composite of the binder and carbon black; Ni^{2+} and Ni^{3+} peaks could not be obtained. However, etching into an ~ 8 nm depth led to well-resolved Ni^{2+} and Ni^{3+} peaks. Change in the oxidation states of Si in SiO_2 was estimated from the peak position, and a reference SiO_2 thin film was used to estimate the etched depth. In this technique, the energy of photoelectrons, ejected when the sample was irradiated by soft X-rays, was analyzed. Because each element has a unique set of binding energies, XPS can be used to identify and determine the concentration of the Ti and Si elements.

Electrochemical impedance spectroscopy data were collected before and after 40 cycles at 60°C (after discharging to 3 V) with an ac amplitude of 10 mV in the frequency range of 0.5 MHz–10 mHz by an Ivium impedance analyzer. We could not ignore the effects from the lithium metal, but its effect on the impedance of the tested cells was believed to be identical because we used the same lithium metal for the cell fabrication. Powder X-ray diffractometer (XRD, D/Max2000, Rigaku) measurements using Cu $\text{K}\alpha$ radiation were used to identify the phase. The surfaces of the uncoated and coated samples were observed using a scanning electron microscope (SEM, JSM 6400, JEOL).

Results and Discussion

Figure 1 shows XRD patterns of the uncoated and SiO_2 -coated samples, showing a typical hexagonal layered structure without any secondary phases. These patterns were nearly identical to that of an uncoated TiO_2 sample. The lattice constants *a* and *c* of the uncoated and 1 wt % SiO_2 - and TiO_2 -coated cathodes annealed at 750°C are shown in Table I. The lattice constants of the TiO_2 -coated cathode show a slight expansion caused by the slightly larger ionic radius of Ti^{4+} (0.605 Å) compared to that of Ni^{3+} (0.56 Å).¹³ This result

* Electrochemical Society Active Member.

^z E-mail: jpcho@unist.ac.kr

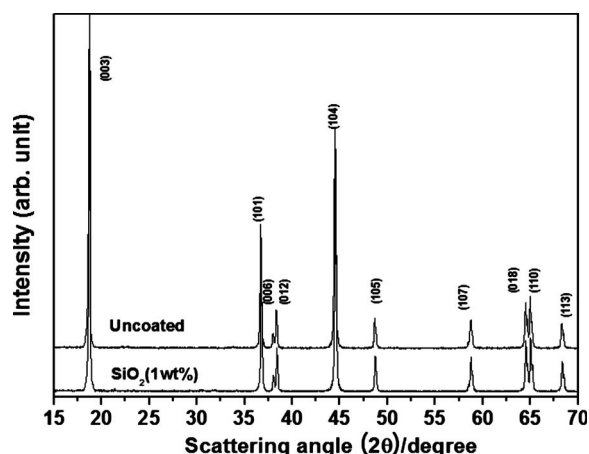


Figure 1. XRD patterns of uncoated and 1 wt % SiO_2 -coated $\text{LiNi}_{0.8}\text{Co}_{0.15}\text{Al}_{0.05}\text{O}_2$ cathode powders.

indicates that TiO_2 may be fully incorporated with the layered structure, thus forming a solid solution throughout the particle. In contrast to the TiO_2 coating, a SiO_2 coating led to no change in the lattice constant, indicating that Si elements are mostly confined near or on the surface areas.

Figure 2 shows typical morphologies of the TiO_2 - and SiO_2 -coated $\text{LiNi}_{0.8}\text{Co}_{0.15}\text{Al}_{0.05}\text{O}_2$ cathode particles. Their surface morphologies are identical to that of an uncoated cathode. An electron probe microanalysis (EPMA) (Fig. 3) of the cross-sectional cathodes of Ti and Si elements shows that Si elements have a higher concentration at the surfaces compared to that of Ti elements (Fig. 3b), which is uniformly distributed throughout the particle. Figure 3d clearly supports the fact that Si is mainly distributed on the surface at a thickness of $\sim 0.5 \mu\text{m}$. Combined XRD and EPMA data confirm that confinement of the Si element in such a thickness did not lead to the change in the lattice constants.

Figure 4 shows the XPS of a SiO_2 -coated cathode while increasing the depth inward the particle. The SiO_2 peak at $\sim 104.5 \text{ eV}$ shifts to a lower energy as the depth increases, indicating that the Si ions ($4+$) in SiO_2 entered lower oxidation states. Si^{4+} ions are very stable but may be vulnerable to turn into lower oxidation states when coated with highly reactive Ni-rich cathodes at 700°C . As can

Table I. XRD lattice constants a and c of uncoated and coated $\text{LiNi}_{0.8}\text{Co}_{0.15}\text{Al}_{0.05}\text{O}_2$ with SiO_2 and TiO_2 .

Material	a ($\pm 0.001 \text{ \AA}$)	c ($\pm 0.002 \text{ \AA}$)
Uncoated	2.863(9)	14.186(4)
TiO_2 (1 wt %)	2.8670(4)	14.193(2)
SiO_2 (1 wt %)	2.863(9)	14.187(4)

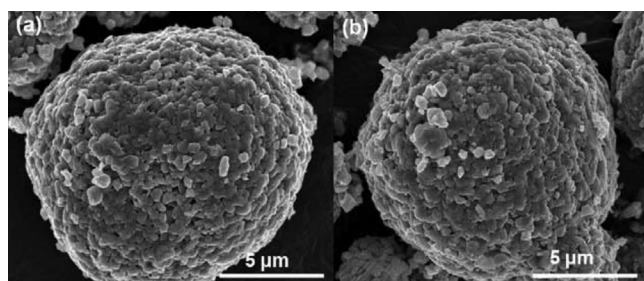


Figure 2. SEM images of (a) uncoated and (b) SiO_2 -coated $\text{LiNi}_{0.8}\text{Co}_{0.15}\text{Al}_{0.05}\text{O}_2$ cathode particles.

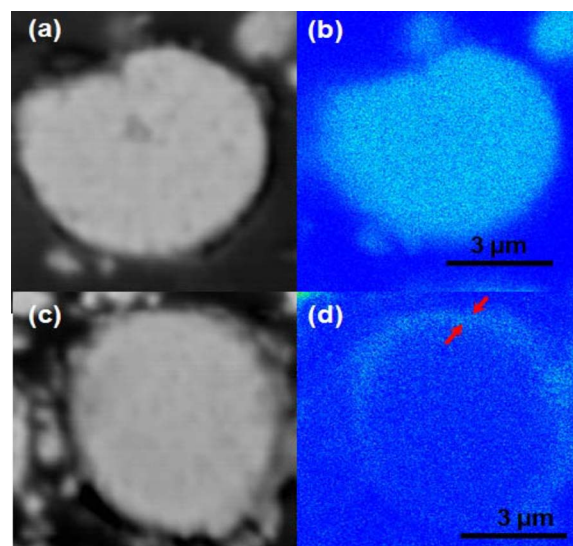


Figure 3. (Color online) (a) SEM image of cross-sectional TiO_2 -coated $\text{LiNi}_{0.8}\text{Co}_{0.15}\text{Al}_{0.05}\text{O}_2$ cathode particle, (b) mapping of Ti elements of (a), (c) SEM image of cross-sectional SiO_2 -coated $\text{LiNi}_{0.8}\text{Co}_{0.15}\text{Al}_{0.05}\text{O}_2$ cathode particle, and (d) mapping of Si elements of (c).

be seen in Fig. 3d, Si elements are partially observed even in the core of the particle. Accordingly, some Si elements in the particles are believed to be incorporated into metal sites (3b) in the cathode. The SiO_2 -coated $\text{LiNi}_{0.8}\text{Co}_{0.2}\text{O}_2$ cathode obtained from the decomposition of SiH_4 at 300°C demonstrated the presence of both Si^{4+} and Si^{2+} ions based upon XPS analysis.² However, they did not report the depth profile of a Si element.

Figure 5 shows voltage profiles of uncoated and TiO_2 - and SiO_2 -coated cathodes at 0.1, 0.2, 0.5, and 1C (3.8 mA/cm^2) rates in coin-type half-cells at 60°C , along with the discharge capacities at each rate. Their discharge capacities, capacity retention, and coulombic efficiencies are summarized in Table II. The SiO_2 coating led to a first discharge capacity of 172 mAh/g , showing a decrease in this capacity of 10 mAh/g . However, the SiO_2 coating improved the coulombic efficiency by 2% compared to the uncoated sample. In addition, the discharge capacity of the coated sample at a 1C rate was 153 mAh/g . Upon cycling at 60°C at a 1C rate, the discharge capacity of the uncoated cathode decreased rapidly, settling at 41 mAh/g after 40 cycles, whereas the SiO_2 -coated cathode was 101 mAh/g . Although the TiO_2 -coated cathode also exhibited an im-

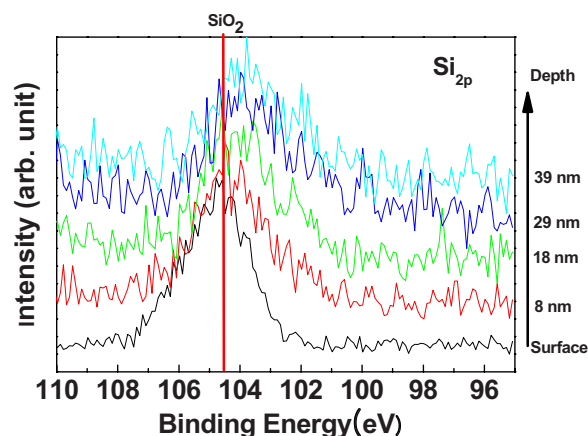


Figure 4. (Color online) XPS spectra of Si 2p in the SiO_2 -coated electrodes with increasing depth from the surface.

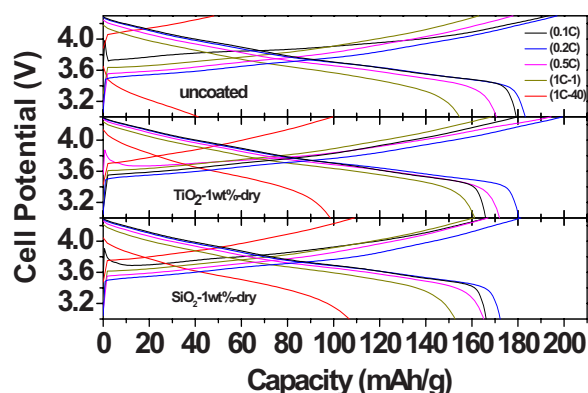


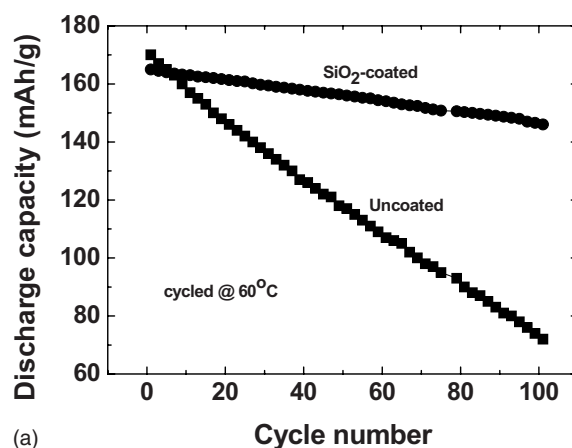
Figure 5. (Color online) Voltage profiles of uncoated and TiO_2 - and SiO_2 -coated $\text{LiNi}_{0.8}\text{Co}_{0.15}\text{Al}_{0.05}\text{O}_2$ cathodes with increasing C rates from 0.1C to 1C in lithium cells at 60°C . At 1C rate ($3.8 \text{ mA}/\text{cm}^2$), the cells were cycled for 40 cycles.

proved capacity retention compared to the uncoated sample, its performance after cycling was inferior to that of the SiO_2 -coated sample.

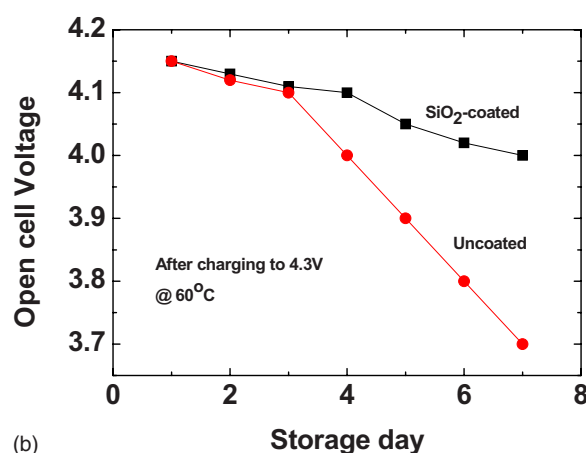
Figure 6a shows the discharge capacity of the uncoated and coated samples as a function of cycle number at 60°C in lithium cells at a rate of 0.5C. The result shows a vivid difference between the uncoated and SiO_2 -coated samples and is quite similar to the cycling data at 60°C at a rate of 1C. After charging the cell, open cell voltage (OCV) was monitored in Fig. 6b using lithium cells during storage at 60°C . The coated sample shows a smaller voltage drop than the uncoated one after 7 days. To elucidate the superior electrochemical performance of the SiO_2 -coated sample to the uncoated one at 60°C , impedance spectra measurements were carried out.

Figure 7 shows the impedance spectra of the uncoated and TiO_2 - and SiO_2 -coated samples before and after 40 cycles at a rate of 1C at 60°C . An equivalent circuit was used to interpret the impedance results (Fig. 7a). R_o and R_{sf} are the ohmic resistance of the cell and the surface film resistance, respectively. R_{ct} is the charge-transfer resistance at the electrode and electrolyte. Compared to the uncoated sample, the SiO_2 -coated sample showed greatly decreased values of R_{ct} and R_{SEI} . As shown in Table III, the R_{sf} and R_{ct} values of the uncoated sample are nearly 16 times larger than those of the SiO_2 -coated sample after cycling. The resistance values of the TiO_2 -coated sample are much smaller than those of the uncoated sample but are larger than those of the SiO_2 -coated sample. Increased surface film and charge-transfer resistances are indicative of forming a larger fraction of the nonconducting interfacial films as a result of enhanced side reactions with the electrolytes. Concomitant with this phenomenon, self-discharge occurred due to the loss of lithium ions from the lattice, which led to a continuous voltage drop during storage. In this regard, SiO_2 coating is very effective in decreasing the side reactions.

Figure 8 shows the XPS spectra of the uncoated and SiO_2 -coated cathode before and after cycling at 60°C at a depth of 8 nm from the surface; the spectra of the uncoated cathode were quite similar to



(a)



(b)

Figure 6. (Color online) Plots of (a) discharge capacity vs cycle number and (b) OCV of uncoated and SiO_2 -coated $\text{LiNi}_{0.8}\text{Co}_{0.15}\text{Al}_{0.05}\text{O}_2$ cathodes in lithium half-cells at 60°C . The cells were cycled for 100 cycles at a 0.5C rate ($1.9 \text{ mA}/\text{cm}^2$). For a storage test, charged lithium cells were stored at 60°C for 7 days.

those of the SiO_2 -coated one before cycling. The spectra of the cathodes between 859 and 852 eV can be deconvoluted into Ni^{2+} and Ni^{3+} peaks and were converted to their relative peak area. In all Ni-based cathode materials dealing with XPS, there was no assignment on the peak at $\sim 860 \text{ eV}$. In our case, both uncoated and coated samples display peaks at $\sim 860 \text{ eV}$, although there are intensity variations. The X-rays penetrate the surface to depths that exceed those surface layers responsible for photoelectric and Auger electrons in an XPS spectrum. Electrons emitted within the sample may undergo inelastic collisions, thus altering the energy of the electron recorded by the detection system. These energy loss processes result in a background of counts that are derived from electronic states other than the characteristic energies for the photoelectric lines, but, moreover, the shape of the background takes on a character determined by the probability distribution for electrons with a given kinetic energy undergoing some modifications to their

Table II. Discharge capacities at various C rates in the uncoated and coated cathodes at a rate of 1C under 60°C cycling. After 1 cycle at a 0.1C rate, the cells were cycled at a 1C rate for 30 cycles.

	0.1C (Q^a)	0.2C	0.5C	1C-1st	1C-40th (1C-40th/1C-1st % ^a)
Uncoated	182(93)	180	170	154	41(27)
1 wt % TiO_2	179(90)	171	166	160	98(61)
1 wt % SiO_2	172(95)	166	165	153	109(70)

^a Q indicates coulombic efficiency.

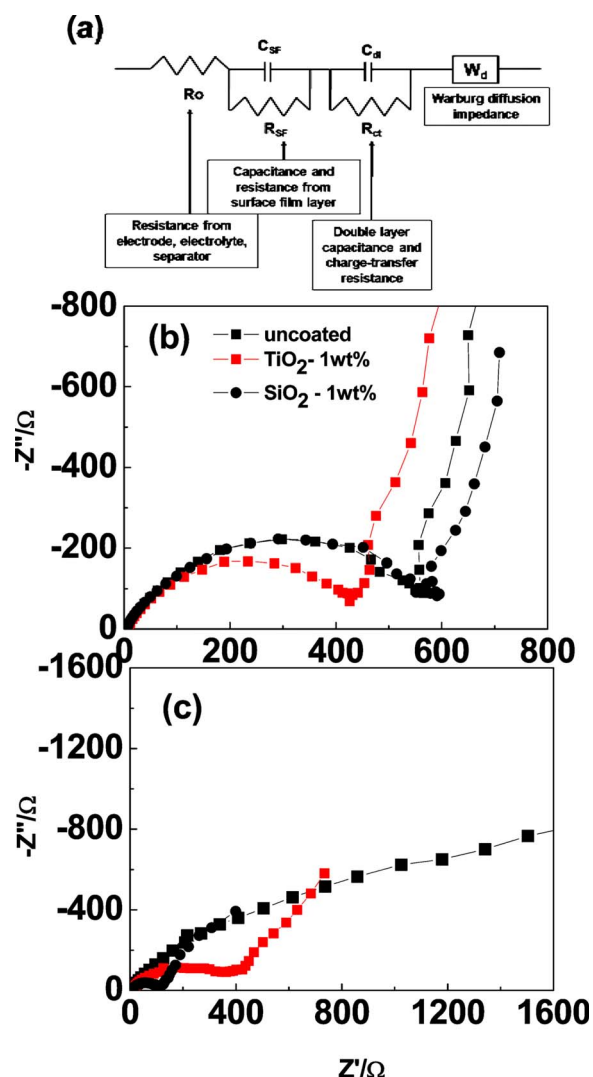


Figure 7. (Color online) (a) Equivalent circuit and impedance spectra (b) before and (c) after 40 cycles at 60°C in uncoated and SiO₂- and TiO₂-coated electrodes in coin-type half-cells. Tests were carried out after fully discharging to 3 V.

initial value.¹⁴ If this probability distribution also exhibits a resonance-type structure, the convolution of a photoelectric peak with this bias in the energy loss distribution may give rise to peak-like structures that may be considered part of the background. That is, peaks at ~860 eV may appear in the XPS spectra, which are actually extrinsic in nature rather than intrinsic to the photoexcitation mechanism.

The formation of Ni²⁺ species is likely caused by the spontaneous reduction from Ni³⁺ ions; for instance, NiO formation in conjunction with a loss of oxygen in the lattice is very well known in a Ni-rich system.^{15,16} Here, even after coating, the originally present Ni²⁺ could not be removed. Figure 9 shows the variation in the relative area percentage of Ni²⁺ and Ni³⁺. Before cycling, Ni³⁺ spe-

Table III. Resistance values of uncoated and coated cathodes after cycling at 60°C at a rate of 1C for 40 cycles.

	R_o	R_{SEI}	R_{ct}
Uncoated	5	795	900
1 wt % TiO ₂	5	90	260
1 wt % SiO ₂	5	50	55

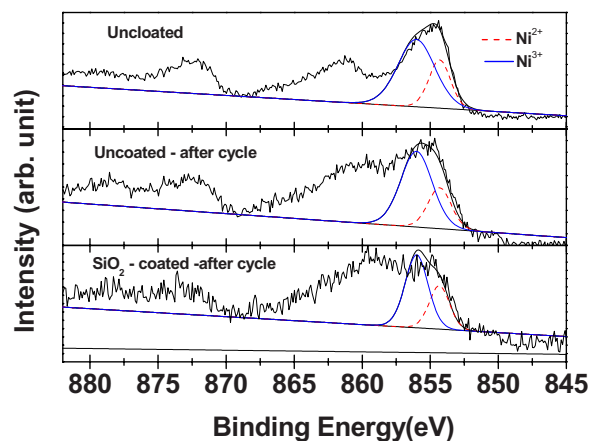


Figure 8. (Color online) XPS spectra of Ni 2p_{3/2} in uncoated and SiO₂-coated electrodes before and after 60°C cycling.

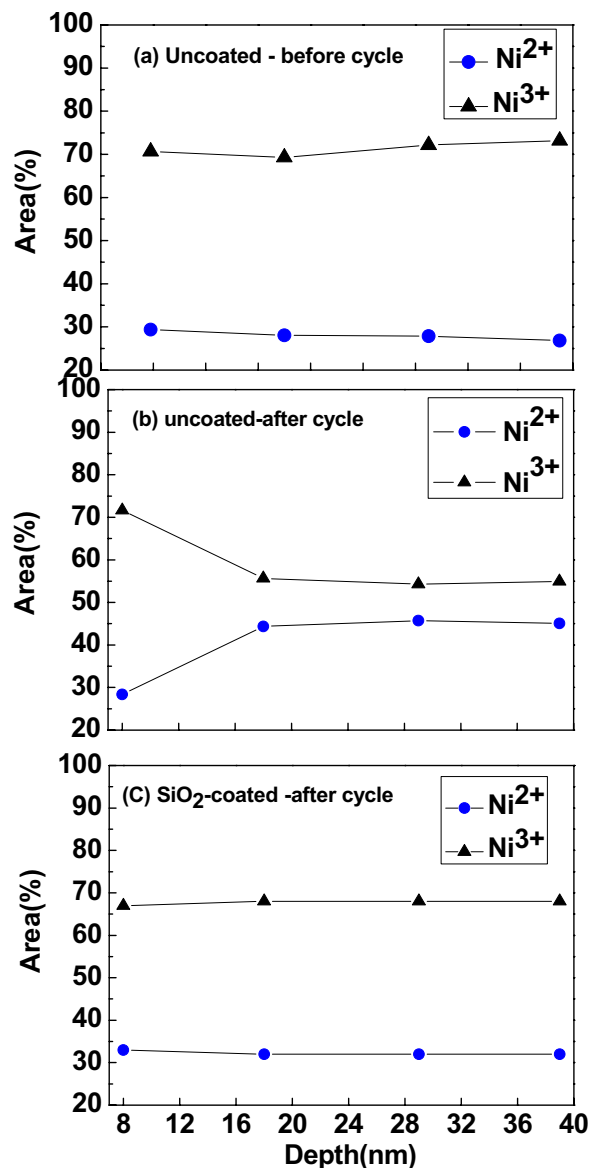


Figure 9. (Color online) Plot of relative area of Ni²⁺ and Ni³⁺ peaks in the uncoated and SiO₂ cathode electrodes before and after 60°C cycles.

cies are dominant, showing >70%. After cycling at 60°C, relative areas of Ni³⁺ and Ni²⁺ at a depth of 8 nm are similar to those before cycling, and Ni²⁺ species rapidly increase to a depth of 18 nm, after which it remains flattened to 40 nm. The Ni³⁺ peak shows an opposite trend to Ni²⁺. This result indicates that an increase in the fraction of Ni²⁺ species is accelerated with sacrificing Ni³⁺ species under cycling at 60°C. These Ni²⁺ species may have originated from the reduction of Ni³⁺ and Ni⁴⁺ surface species.¹⁷ However, the fractions of Ni²⁺ and Ni³⁺ species in the SiO₂-coated cathode after cycling are similar to those of the uncoated cathode before cycling. Impedance and XPS results indicate that the localized presence of Si elements on the surface diminishes reactions with the electrolytes with Ni³⁺ species at 60°C.

Conclusion

Dry coating using SiO₂ nanoparticles on LiNi_{0.8}Co_{0.15}Al_{0.05}O₂ led to a dominant distribution of Si elements near the surface, in contrast to what was observed with a TiO₂ coating. This localized distribution of Si elements resulted in a greatly improved capacity retention at 60°C. After 40 cycles at a rate of 1C, the capacity retention of the SiO₂-coated sample was 70%, whereas that of the uncoated cathode was 27%. This improvement is due to the localized Si elements near the surfaces, which diminished the formation of Ni²⁺ species at the interfaces.

Acknowledgment

This work was supported by a grant from the Technology Innovation Program of the Ministry of Knowledge Economy of Korea

(project no. 10032319). Also, financial support from World Class University (WCU) program is greatly acknowledged.

Ulsan National Institute of Science and Technology assisted in meeting the publication costs of this article.

References

1. J. Eom, K. S. Ryu, and J. Cho, *J. Electrochem. Soc.*, **155**, A228 (2008).
2. H. Omanda, T. Brousse, C. Marhic, and D. M. Schleich, *J. Electrochem. Soc.*, **151**, A922 (2004).
3. Y. Kim and J. Cho, *J. Electrochem. Soc.*, **154**, A495 (2007).
4. H. Lee, M. G. Kim, and J. Cho, *Electrochem. Commun.*, **9**, 149 (2007).
5. J. Liu and A. Manthiram, *J. Electrochem. Soc.*, **156**, A833 (2009).
6. Y.-K. Sun, S.-T. Myung, C. S. Yoon, and D.-W. Kim, *Electrochem. Solid-State Lett.*, **12**, A163 (2009).
7. H. Lee, Y. Kim, Y.-S. Hong, Y. Kim, M. G. Kim, N.-S. Shin, and J. Cho, *J. Electrochem. Soc.*, **153**, A781 (2006).
8. M. G. Kim and J. Cho, *J. Mater. Chem.*, **18**, 5880 (2008).
9. M. G. Kim and J. Cho, *Adv. Funct. Mater.*, **19**, 1497 (2009).
10. J. Eom, M. G. Kim, and J. Cho, *J. Electrochem. Soc.*, **155**, A239 (2008).
11. N. Mijung, Y. Lee, and J. Cho, *J. Electrochem. Soc.*, **153**, A935 (2006).
12. Y. Ito and Y. Ukyo, *J. Power Sources*, **146**, 39 (2005).
13. R. D. Shannon and C. T. Prewitt, *Acta Crystallogr., Sect. A: Cryst. Phys., Diffraction, Theor. Gen. Crystallogr.*, **32**, 751 (1976).
14. <http://www.casaxps.com>, last accessed June 18, 2009.
15. S. Liu, Z. R. Zhang, Z. L. Gong, and Y. Yang, *Electrochem. Solid-State Lett.*, **7**, A190 (2004).
16. J. Li, J. M. Zheng, and Y. Yang, *J. Electrochem. Soc.*, **154**, A427 (2007).
17. A. M. Andersson, D. P. Abraham, R. Haasch, S. MacLaren, J. Liu, and K. Amine, *J. Electrochem. Soc.*, **149**, A1358 (2002).